THE JOURNAL OF BIOLOGICAL CHEMISTRY VOL. 284, NO. 29, pp. 19482–19492, July 17, 2009

Constitutive and Regulated Endocytosis of the Glycine Transporter GLYT1b Is Controlled by Ubiquitination*[S]

Received for publication, April 7, 2009, and in revised form, May 22, 2009 Published, JBC Papers in Press, May 27, 2009, DOI 10.1074/jbc.M109.005165

Enrique Fernández-Sánchez, Jaime Martínez-Villarreal, Cecilio Giménez, and Francisco Zafra[1]

From the Centro de Biología Molecular "Severo Ochoa," Facultad de Ciencias, Universidad Autónoma de Madrid, Consejo Superior de Investigaciones Científicas, Centro de Investigación en Red de Enfermedades Raras, Madrid 28049, Spain

The glycine transporter GLYT1 regulates both glycinergic and glutamatergic neurotransmission by controlling the reuptake of glycine at synapses. Trafficking of GLYT1 to and from the cell surface is critical for its function. Activation of PKC down-regulates the activity of GLYT1 through a mechanism that has so far remained uncharacterized. Here we show that GLYT1b undergoes fast constitutive endocytosis that is accelerated by phorbol esters. Both constitutive and regulated endocytosis occur through a dynamin 2- and clathrin-dependent pathway, accumulating in the transporter in transferrin-containing endosomes. A chimera with the extracellular and transmembrane domains of the nerve growth factor receptor and the COOH-terminal tail of GLYT1 was efficiently internalized through this clathrin pathway, suggesting the presence of molecular determinants for GLYT1b endocytosis in its COOH-terminal tail. Extensive site-directed mutagenesis in this region of the chimera highlighted the involvement of lysine residues in its internalization. In the context of the full-length transporter, lysine 619 played a prominent role in both the constitutive and phorbol 12-myristate 13-acetate-induced endocytosis of GLYT1b, suggesting the involvement of ubiquitin modification of GLYT1b during the internalization process. Indeed, we show that GLYT1b undergoes ubiquitination and that this process is stimulated by phorbol 12-myristate 13-acetate. In addition, this endocytosis is impaired in an ubiquitination-deficient cell line, further evidence that constitutive and regulated endocytosis of GLYT1b is ubiquitin-dependent. It remains to be determined whether GLYT1b recycling might be affected in pathologies involving alterations to the ubiquitin system, thereby interfering with its influence on inhibitory and excitatory neurotransmission.

Glycine fulfills a dual role in neurotransmission by mediating inhibition through the strychnine-sensitive glycine receptor and excitation as a co-agonist of the NMDA[2] receptors (1, 2). Although it was initially believed that the concentration of glycine in the synaptic cleft would be sufficient to saturate the glycine sites on NMDA receptors, recent pharmacological and electrophysiological evidence indicates that due to the activity of the GLYT1 (glycine transporter-1) glycine transporter, this is probably not the case. Three isoforms of GLYT1 exist that differ in their NH_2-terminal sequence (GLYT1a, GLYT1b, and GLYT1c), and they are strongly expressed in glycinergic areas of the nervous system, predominantly in glial cells (3). Indeed, mice lacking GLYT1 have impaired glycinergic neurotransmission, which has been attributed to an increase in extracellular glycine close to the strychnine-sensitive glycine receptor (4). Moreover, GLYT1 has been identified in neuronal elements closely associated with the glutamatergic pathways throughout the brain (5, 6). GLYT1 is enriched in presynaptic buttons, where it largely co-localizes with the vesicular glutamate transporter vGLUT1. It is also present in the postsynaptic densities of asymmetric synapses, and complexes containing both NMDA receptor and GLYT1 have been shown to exist (5). In these postsynaptic sites, the distribution of GLYT1 is partially controlled through its interaction with the scaffolding protein PSD-95 (7). Accordingly, GLYT1 is believed to play a role in controlling the concentration of glycine in the microenvironment around the NMDA receptor. Indeed, functional studies have shown that a specific GLYT1 inhibitor, *N*-[3-(4′-fluorophenyl)-3-(4′-phenylphenoxy)propyl]sarcosine, potentiates NMDA-mediated responses *in vitro* and *in vivo* (8–10). The potential role of GLYT1 in glutamatergic neurotransmission has also been confirmed in heterozygous $Glyt1^{+/-}$ animals that express only 50% of the normal levels of GLYT1 as well as when GLYT1 expression is disturbed in forebrain neurons. In these animals, hippocampal NMDA receptor function is enhanced, and the mice appear to display better memory retention than wild type mice (11–13).

The mechanisms responsible for the insertion of GLYT1 into glutamatergic synapses are unknown. However, recent studies indicate that the movement of transporters within the cell is highly organized and that a number of ancillary proteins control their intracellular trafficking by interacting with targeting motifs in the transporter. Indeed, like other neurotransmitter transporters, GLYT1 is asymmetrically distributed in polarized cells (14, 15). The asymmetric distribution of sodium-dependent neurotransmitter transporters (NSS) requires a number of steps that commence with their efficient exit from the endo-

* This work was supported by Spanish Dirección General de Investigación Científica y Técnica Grant SAF2008-01059, a grant from the Fondo de Investigaciones Sanitarias (CIBERER), a grant from the Comunidad Autónoma de Madrid, and an institutional grant from the Fundación Ramón Areces.

[S] The on-line version of this article (available at http://www.jbc.org) contains supplemental Figs. S1–S3.

[1] To whom correspondence should be addressed: Centro de Biología Molecular "Severo Ochoa," Universidad Autónoma de Madrid, C/Nicolas Cabrera 1, Madrid 28049, Spain. Tel.: 34-911964630; Fax: 34-911964420; E-mail: fzafra@cbm.uam.es.

[2] The abbreviations used are: NMDA, *N*-methyl-D-aspartic acid; PKC, protein kinase C; PMA, phorbol 12-myristate 13-acetate; DAT, dopamine transporter; GFP, green fluorescent protein; MDCK, Madin-Darby canine kidney; NGFR, nerve growth factor receptor; YFP, yellow fluorescent protein; HA, hemagglutinin; Ub, ubiquitin; E1, ubiquitin-activating enzyme; Sulfo-NHS-SS-Biotin, sulfosuccinimidyl 2-(biotinamido)-ethyl-1,3-dithiopropionate.

plasmic reticulum. This is followed by sorting processes in the Golgi complex, insertion into the plasma membrane, and the retention of the transporter at functional synaptic sites. Moreover, the amount of transporter in the plasma membrane is also regulated by endocytosis and recycling mechanisms. Like several other members of the NSS family, GLYT1 is subjected to regulation by protein kinase C. Activation of PKC by phorbol esters down-regulates GLYT1, which is endocytosed from the plasma membrane to intracellular compartments in several cell lines (16–18). For years, the molecular mechanisms that mediate phorbol 12-myristate 13-acetate (PMA)-stimulated endocytosis of the NSS family members have remained elusive. However, recent evidence obtained for the dopamine transporter (DAT) has revealed the importance of ubiquitination of DAT for its endocytosis (19). DAT is ubiquitinated by the Nedd4-2 ligase at several intracellular lysines. Indeed, mutation of these lysines abolished both ubiquitination and phorbol ester-stimulated endocytosis, indicating that the associated ubiquitin molecules serve as a platform to recruit endocytotic adaptors (20–23). Ubiquitination has also been implicated in the endocytosis of other membrane proteins, including the main transporter for glutamate, GLT1, and the system A transporter SNAT2 (24–26).

Ubiquitin coupling can involve either mono- or polyubiquitination. Monoubiquitination occurs when a single ubiquitin molecule is coupled to one or more lysine residues on a target protein, such that the final stoichiometry is one ubiquitin per lysine. Polyubiquitination refers to the coupling of a chain of ubiquitins to a lysine on the target protein, with a final stoichiometry of four or more ubiquitins per lysine. Whereas monoubiquitinated proteins are degraded in lysosomes, polyubiquitinated proteins are recognized by and subsequently degraded by the 26 S proteasome (27).

In this study, we show that GLYT1b is endocytosed through a clathrin-dependent mechanism, a process that is accelerated by phorbol esters. Through a mutational analysis, we have identified a lysine residue in the COOH-terminal tail of the protein as the major determinant for GLYT1b internalization through both constitutive and PMA-stimulated pathways. Ubiquitination GLYT1b is stimulated by PMA, a finding compatible with ubiquitin being the platform on which the clathrin network is assembled.

EXPERIMENTAL PROCEDURES

Materials—The [^{3}H]glycine, protein standards for SDS-PAGE (Rainbow markers), and the ECL Western blotting detection reagents were all obtained from Amersham Biosciences. The Lipofectamine 2000 and pCDNA3 plasmid were purchased from Invitrogen, whereas phenylmethanesulfonyl fluoride, the Expand High Fidelity PCR system, and all restriction enzymes were obtained from Roche Applied Science. The QuikChange site-directed mutagenesis kit used was from Stratagene (La Jolla, CA), the nitrocellulose membranes were obtained from Bio-Rad, and the fetal calf serum was supplied by Invitrogen. The monoclonal mouse anti-HA (clone 12CA5) was prepared at the microscopy service of the Centro de Biología Molecular (Madrid, Spain), whereas the Alexa Fluor 488 or Alexa Fluor 594 coupled goat anti-rabbit and goat anti-mouse were from Molecular Probes, Inc. (Eugene, OR), and the mouse monoclonal anti-ubiquitin (P4D1) was from Santa Cruz Biotechnology, Inc. (Santa Cruz, CA). The Vectashield medium was obtained from Vector (Burlingame, CA), and the EZ-link^{TM} sulfo-NHS-SS-biotin was from Pierce. The pGEM-T easy cloning vector was purchased from Promega (Madison, WI), and the oligonucleotides used were synthesized by Isogen Life Science (Utrech, The Netherlands). All other chemicals were obtained from Sigma.

Cell Growth and Transfection—MDCK cells (American Type Culture Collection) were grown in high glucose Dulbecco's modified Eagle's medium supplemented with 10% fetal bovine serum at 37 °C and in an atmosphere of 5% CO_2. Transient expression in MDCK cells was achieved using Lipofectamine 2000 according to the manufacturer's instructions. The cells were incubated for 48 h at 37 °C and then analyzed biochemically or by immunofluorescence and/or in transport assays.

Plasmid Constructs—The various GLYT1 mutants used in this study were prepared using the rat GLYT1b cDNA (7) as a template and the QuikChange^{TM} site-directed mutagenesis kit, according to the manufacturer's instructions. Previously, an HA tag was included in the NH_2 terminus of the transporter by PCR or the YFP in the COOH terminus, as described previously (28). The inclusion of these tags had no effect either on the activity or on the subcellular distribution of the transporter. All of the mutations were confirmed by sequencing of the clones.

Transport Assays—[^{3}H]Glycine transport in transfected cells was measured as described previously (29).

Protein Determination—Protein concentrations were determined with the Bio-Rad protein determination kit and using bovine serum albumin as the standard.

Cell Surface Biotinylation—Cells were plated at 50% confluence in 60-mm cell culture plates and transfected as indicated above. After 2 days, the cell surface proteins were labeled with the non-permeable sulfo-NHS-SS-biotin reagent as described previously (28).

Isolation of GLYT1-His-Ubiquitin Conjugates—MDCK cells were grown in p100 dishes, and they were then transfected with expression vectors for GLYT1b-YFP and His-Ub. Two days later, the cells were lysed in 2 ml of buffer (6 M guanidium HCl, 0.1 M Na_2HPO_4/NaH_2PO_4, pH 8.0, 5 mM imidazole), sonicated for 2 min, and incubated with 70 μl of Ni^{2+}-nitrilotriacetic acid-agarose beads for 4 h at room temperature with rotatory agitation. The beads were collected by mild centrifugation and washed exhaustively with the sequential addition of 1) 340 μl of 6 M guanidium HCl 0.1 M sodium phosphate, pH 8.0; 2) 700 μl of 6 M guanidium HCl, 0.1 M sodium phosphate, pH 5.8; 3) 340 μl of 6 M guanidium-HCl, 0.1 M sodium phosphate, pH 8.0; 4) 700 μl of 1:1 6 M guanidium HCl, 0.1 M sodium phosphate, pH 8.0, 50 mM sodium phosphate, 100 mM KCl, 20% glycerol, 0.2% Nonidet P-40; 5) 700 μl of 1:3 6 M guanidium HCl, 0.1 M sodium phosphate, pH 8.0, 50 mM sodium phosphate, 100 mM KCl, 20% glycerol, 0.2% Nonidet P-40; 6) 700 μl of 50 mM sodium phosphate, 100 mM KCl, 20% glycerol, 0.2% Nonidet P-40; and 7) the last solution with 10 mM imidazole. Finally, the protein was eluted with 30 μl of the final wash solution containing 500 mM imidazole, and the proteins recovered were analyzed by SDS-PAGE and immunoblotting.

Electrophoresis and Immunoblotting—SDS-PAGE was carried out on 7.5% polyacrylamide gels in the presence of 2-mercaptoethanol. After electrophoresis, the protein samples were transferred to a nitrocellulose membrane, as described previously (28). The blot was then probed overnight at 4 °C with the primary antibody (anti-HA or anti-ubiquitin), which was then detected after washing with an anti-mouse IgG peroxidase-linked secondary antibody. The labeled bands were visualized by ECL and quantified by densitometry (Molecular Dynamics ImageQuant version 3.0).

Immunofluorescence in Cultured Cells—MDCK cells grown on glass coverslips were transfected with the corresponding expression vectors using Lipofectamine 2000, according to the manufacturer's instructions. Immunostaining was performed as described previously (26). Antibody staining was visualized, and the images were captured on confocal microradiance equipment (Bio-Rad) coupled to an Axioscop2 microscope (Carl Zeiss, Jena, Germany).

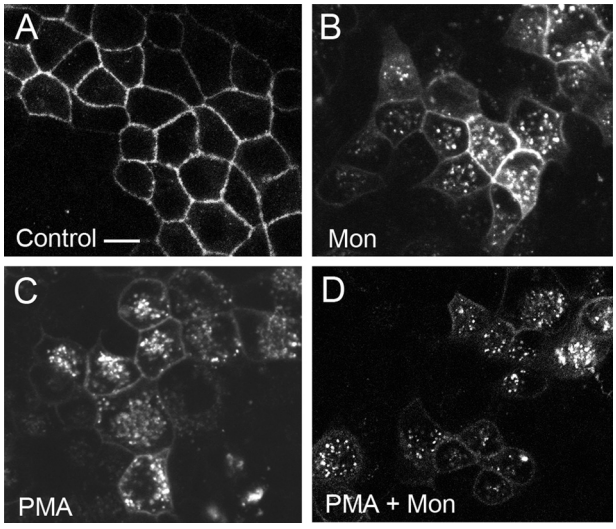

FIGURE 1. **PMA and monensin promote the internalization of GLYT1b-YFP.** MDCK cells were transfected with GLYT1b-YFP, and 2 days later they were exposed to the vehicle alone (*A*), monensin (10 μM, 30 min) (*B*), or PMA (1 μM, 30 min) (*C*), or both of these compounds together (*D*). The cells were then fixed with 4% paraformaldehyde and analyzed by confocal microscopy (*scale bar*, 15 μm).

RESULTS

GLYT1b Is Endocytosed by a Clathrin-dependent Mechanism—To study the endocytosis of GLYT1b, we mainly used the MDCK cell line in which the transfected transporter is efficiently exported to the cell surface, thereby avoiding any interference of the intracellular biosynthetic intermediates in the microscopy analysis (Fig. 1*A*). The presence of GLYT1b in the cell surface was confirmed in preliminary experiments by measuring [^{3}H]glycine uptake in transfected cells. This localization is also supported (with the limitations imposed by the resolution limit of the confocal microscope) by colocalization of this transporter with the β-subunit of the Na^+K^+-ATPase, a marker of the plasma membrane. To more rapidly detect the protein, a YFP-tagged construct was used, although similar results were obtained with the HA-tagged GLYT1b or the untagged transporter (compare Fig. 1 with Fig. 4*D*) (data not shown). A common technique to investigate the constitutive endocytosis of membrane proteins consists of blocking protein recycling to the plasma membrane with the carboxylic ionophore monensin (20, 30–33). This treatment inhibits transport through acidic endosomes and, consequently, the recycling of proteins to the plasma membrane, promoting the accumulation of the endocytosed protein in endosomes. Exposing MDCK cells transiently transfected with GLYT1b-YFP to a non-toxic concentration of monensin (10 μM) promoted the accumulation of the transporter in intracellular vesicular structures in conjunction with a decrease in the amount of the transporter at the cell surface (Fig. 1*B*). Similarly, treatment of MDCK cells with the protein kinase C activator PMA induced the accumulation of GLYT1b-YFP in vesicles concomitant with a reduction in the expression of this protein in the plasma membrane region (Fig. 1*C*). Indeed, simultaneous exposure of the cells to both PMA and monensin further increased the intracellular accumulation of GLYT1b-YFP (Fig. 1*D*).

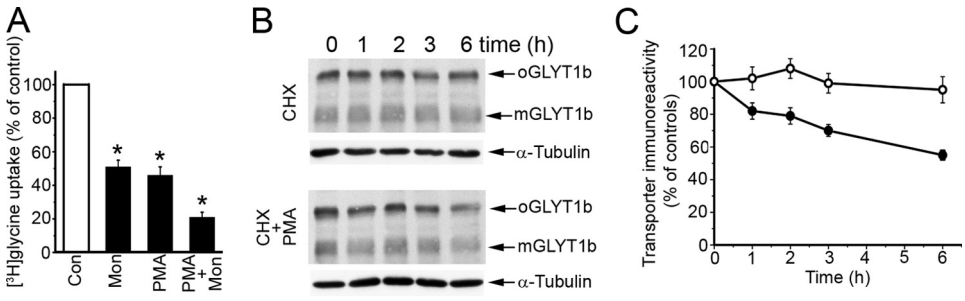

FIGURE 2. **Effect of PMA and monensin on glycine uptake and stability of GLYT1b.** *A*, MDCK cells were transfected with GLYT1b-YFP, and 2 days later, [^{3}H]glycine uptake was measured for 10 min in cells pretreated for 30 min before the uptake assay with the vehicle alone (*Con*), with monensin (10 μM) (*Mon*), with PMA (1 μM), or with both of these compounds together (*Mon* + *PMA*). The results represent the means ± S.E. of three triplicate determinations, and they are presented as a percentage of the controls. Values were compared with control values by using Student's *t* test. *, $p < 0.001$. *B*, MDCK cells were transfected with GLYT1b-YFP, and 2 days later they were preincubated for 2 h in the presence of cycloheximide (50 μM). Incubation continued for the indicated times in the presence of cycloheximide (*CHX*; 50 μM) or cycloheximide plus PMA (*CHX* + *PMA*; 50 μM and 1 μM, respectively). Cellular extracts were resolved by SDS-PAGE and analyzed by immunoblotting with anti-GFP antibody. Bands corresponding to monomers (*mGLYT1b*) and oligomers (*oGLYT1*) are indicated by *arrows*. As a loading control, blots were reprobed with anti-α-tubulin. Note that due to the abundance of α-tubulin, exposure times were shorter for this protein than for GLYT1-YFP. *C*, bands corresponding to monomers and to oligomers in *B* were quantified by densitometry. Densitometry values of both bands were added and represented as a percentage of the densitometry values at time 0. Values are the means ± S.E. of three experiments. ○, cycloheximide; ●, cycloheximide plus PMA.

The loss of functional GLYT1b from the surface of cells exposed to monensin- and PMA was confirmed by assessing the [^{3}H]glycine uptake in MDCK cells transfected with GLYT1b (Fig. 2*A*). When compared with untreated controls, a 30-min exposure to monensin produced a 49% reduction in glycine uptake, measured over 10 min, whereas PMA induced a 54% reduction. Simultaneous exposure to both reagents further reduced uptake up to 79%. Nevertheless, it should be noted that a fraction of the meas-

ured effect of monensin on glycine uptake might be due to an indirect disruption of the sodium gradients.

These experiments suggested that there was a constitutive pathway to remove GLYT1b from the cell surface to the intracellular compartment (visualized only in the presence of monensin), which was accelerated by exposure to PMA. Alternatively, PMA might inhibit the insertion of the transporter into the membrane. To investigate whether the internalized protein was targeted for degradation or if it was recycled to the cell surface, we analyzed the stability of the protein in these cells. Accordingly, we quantified the amount GLYT1b in the cell extracts when protein synthesis was blocked with cycloheximide, either in the presence or absence of PMA (Fig. 2*B*). These results revealed that in the absence of PMA, the protein was quite stable, and after 6 h, the amount of GLYT1b in the cells decreased by only 5% (Fig. 2*C*). Exposure to PMA accelerated the degradation of GLYT1b, and after 6 h, the amount of this protein had fallen by 42% (Fig. 2*C*). In transfected cells treated with monensin or with PMA, a significant pool of the intracellular GLYT1b-YFP co-localized with a marker of the early/recycling endosome, Texas Red-transferrin (not shown), as also occurred when the cells were exposed to both compounds together (Fig. S1). Accordingly, these treatments appeared to promote the accumulation of GLYT1b-YFP in the early and/or recycling endosome.

Because the aforementioned immunofluorescence and transport assays reflect the steady state, the decrease in transporter at the plasma membrane and the concomitant accumulation in intracellular vesicles might be a consequence of the slower insertion of the transporter into the plasma membrane rather than an acceleration of endocytosis. To directly measure the internalization of GLYT1b from the plasma membrane, we first introduced an extracellular epitope into GLYT1b as previously reported for similar proteins (21), but this transporter proved to be inactive. As an alternative approach, we generated a chimeric protein that consisted of the extracellular and transmembrane domains of the p75 NGFR fused to the NH_2 terminus of GLYT1b (named NG1wt; scheme in Fig. 3*A*). This protein was expressed at the cell surface, and it was fully functional in glycine transport assays, indicating that the GLYT1b part of the chimera was correctly folded (data not shown). Prior to performing the endocytosis assays, the chimera could be labeled at the cell surface of living cells (Fig. 3*B*). To that end, intracellular trafficking was blocked by maintaining the cells at 4 °C, and the chimera at the membrane was then incubated with an antibody against the extracellular domain of NFGR and a fluorescent secondary antibody (Fig. 3, *A* and *B*). When trafficking was restored at 37 °C, the labeled NG1wt chimera was seen to internalize. Thus, after 15 min at 37 °C, a number of intracellular vesicles could already be detected (*arrows* in Fig. 3*C*), and by 30 min, most of the labeled protein was in these intracellular vesicles (constitutive endocytosis) (Fig. 3*D*). To investigate whether PMA accelerated the endocytosis of NG1wt, the cells were exposed to this drug for 15 min, conditions in which the chimera was completely internalized (constitutive plus regulated endocytosis) (Fig. 3*E*). The vesicles with the chimera also co-stained with transferrin in a double labeling endocytosis assay either under constitutive endocytosis or after the PMA treatment (Fig. S2), suggesting that NG1wt and GLYT1b-YFP use the same endocytotic pathway for recycling through the endosomes. To determine whether this internalization was clathrin-dependent, endocytosis of the NG1wt was measured in the presence of hypertonic sucrose. This treatment completely suppressed endocytosis of the chimera either in the presence (Fig. 3*F*) or absence of PMA (Fig. 3*G*). Moreover, the endocytosis of HA-tagged GLYT1b was also dependent on dynamin 2, since the dominant negative mutant of this protein (GFP-tagged mutant K44A) suppressed the endocytosis of HA-GLYT1b in MDCK cells treated with monensin (not shown), with PMA (not shown), or with PMA and monensin simultaneously (Fig. 4, *A–C*). By contrast, wild-type dynamin 2 (GFP tagged) did not affect endocytosis (Fig. 4, *D–F*). PMA- and monensin-promoted internalization of HA-GLYT1b was also blocked in cells transfected with a dominant negative construct of Eps15 (34), another component of clathrin-coated pits (which was GFP-tagged and carried a deletion in residues 95–295) (*G-EPS-*Δ in Fig. 4, *G–I*). A quantitative estimate of the effect of the dynamin 2 dominant negative construct on the PMA-regulated endocytosis was obtained by biotinylation of HA-GLYT1b remaining on the cell surface after the treatment (Fig. 4, *J* and *K*). PMA reduced the amount of cell surface transporter by 60–70% in controls, whereas the reduction was lower than 10% in the presence of Dyn2 K44A (Fig. 4*K*). Further evidence for the involvement of the clathrin-dependent endocytosis was obtained by microscopy analysis of YFP-tagged GLYT1b. Thus, hypertonic sucrose treatment largely abolished the internalization of GLYT1b-YFP in transfected MDCK cells in response to either monensin (Fig. 5, *A* and *B*) or PMA (Fig. 5, *C* and *D*), and few intracellular vesicles were observed after these treatments. Together, these results indicate that GLYT1b underwent active turnover from the plasma membrane to the recycling endosome, a process that was accelerated by activation of the protein kinase C. Moreover, the data support a major contribution of the clathrin-dependent pathway to both the constitutive and the regulated endocytosis of GLYT1b.

Lysine 619, in the Carboxyl-terminal Tail of GLYT1b, Is Required for Constitutive and Regulated Endocytosis—In order to define the GLYT1b residues involved in its clathrin-dependent endocytosis, we searched the transporter sequence for consensus endocytosis motifs. The carboxyl-terminal tail of the transporter was a good candidate to contain such motifs, since it has two dileucine motifs that were previously shown to participate in the basolateral sorting of GLYT1b in MDCK cells and which are also known to be a clathrin recruitment signal in many membrane proteins (35). Moreover, a chimeric construct that contained the extracellular and transmembrane domains of NGFR and with the COOH-terminal tail of GLYT1b substituting for the native COOH-terminal tail of p75 NGFR (named NG1ct-wt; scheme in Fig. S3*A*) was efficiently internalized to the early/recycling endosomes through a clathrin-dependent pathway (see Fig. S3, *B–M*). Consequently, this short chimera was used in initial site-directed mutagenesis studies to define those determinants involved in GLYT1b endocytosis. However, although mutations in the dileucine motifs impaired the internalization of the short chimera, this was not observed later in the full-length protein.

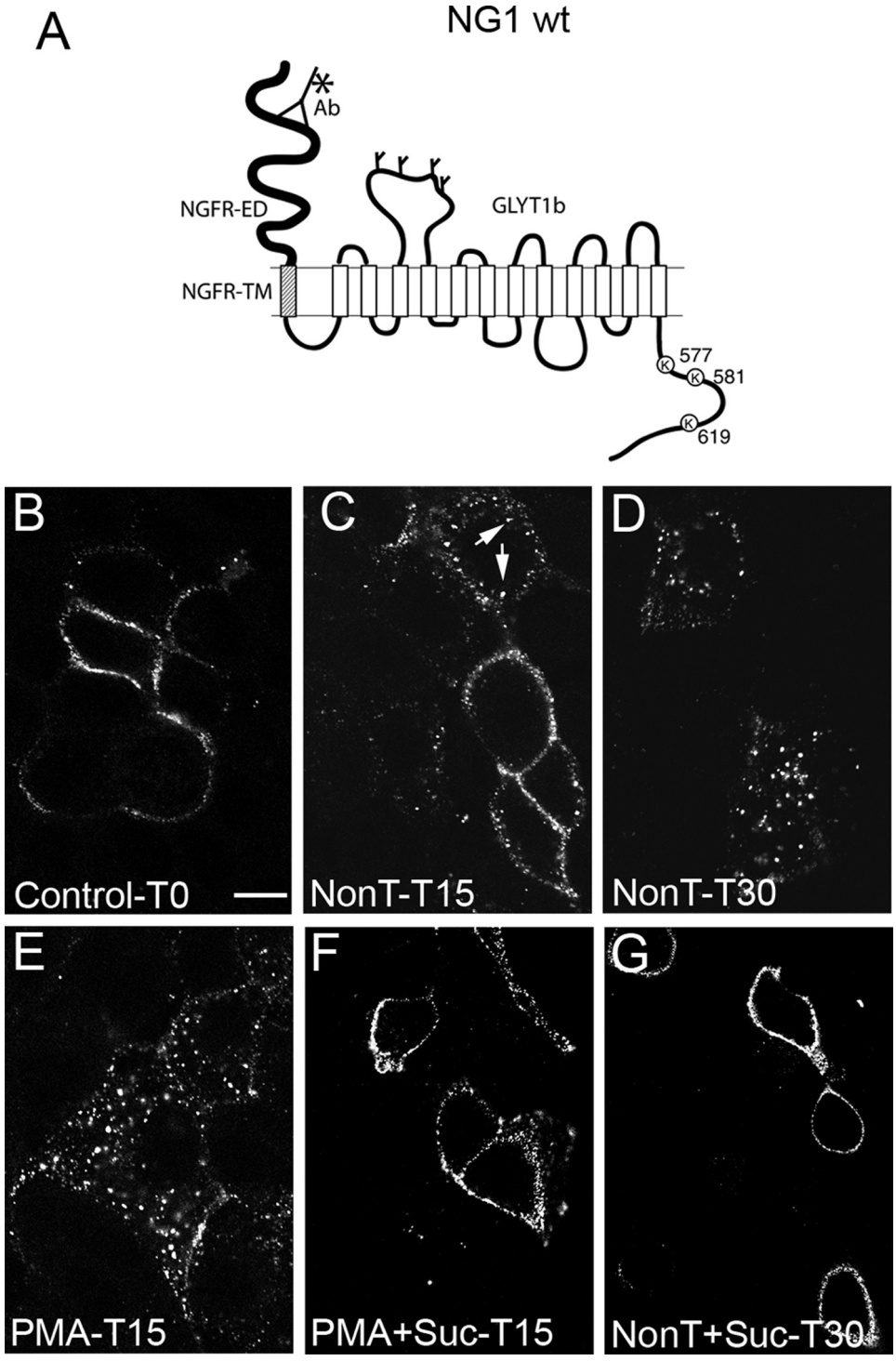

FIGURE 3. **Endocytosis of the NGFR-GLYT1 chimera.** *A*, scheme of the chimeric NG1wt protein constructed with the extracellular and transmembrane domains of the p75 NGFR (*NGFR-ED* and *NGFR-TM*) plus the full-length GLYT1b (*GLYT1b*). The positions of the COOH-terminal lysines mutated in this study are indicated and *numbered* according to GLYT1b. The binding of anti-NGFR (*ab*) to NGFR-ED and that of an Alexa-488-labeled secondary antibody is represented by *Y* and an *asterisk*. *B–G*, MDCK cells were transfected with the full-length chimera NG1wt and labeled at 4 °C with anti-NGFR and the fluorescent secondary antibody. They were then either fixed (*Control-T0* in *B*) or incubated at 37 °C for 15 or 30 min in the presence of the vehicle alone (*NonT-T15* in *C* or *NonT-T30* in *D* and *G*) or 1 μM PMA for 15 min (*PMA-T15* in *E*). In *F* and *G*, the labeled cells were incubated with 0.4 M sucrose for 10 min prior to exposure to PMA for 15 min (*PMA + Suc-T15* in *F*) or the vehicle alone for 30 min (*NonT + Suc-T30* in *G*) in the presence of the sucrose. The cells were then fixed and analyzed by confocal microscopy (*scale bar*, 15 μm).

Since ubiquitin has recently been reported to be involved in the endocytosis of dopamine or glutamate transporters, we also mutated the three lysines present in this domain of GLYT1b (Lys^{577}, Lys^{581}, and Lys^{619}). Internalization of the short chimera was impaired by the simultaneous mutation to arginine of these three lysines (results not shown). To evaluate the contribution of these lysine residues to endocytosis of GLYT1b in the context of the full-length protein, various constructs of GLYT1b-YFP in which these COOH-terminal lysines had been mutated were assayed in MDCK cells. Regarding constitutive endocytosis, after mutation to arginine of the three COOH-terminal lysines, internalization of GLYT1b-YFP to intracellular vesicles was largely blocked in the presence of monensin (Fig. 6*C*; compare with controls in Fig. 6, *A* and *B*), although some vesicles were evident close to the apical surface of MDCK cells (not shown). To investigate whether any one of these lysines might more strongly affect constitutive endocytosis, they were mutated individually or in combination. Furthermore, because GLYT1b also contains two additional lysines in the NH_2 terminus (Lys^{25} and Lys^{26}), we produced constructs in which these residues were also mutated to arginine (mutant K25R/K26R). Mutant 5KR, which lacked NH_2- and COOH-terminal lysines, was endocytosed less than the 3KR mutant in response to monensin, although it was difficult to obtain a quantitative estimate on the basis of fluorescence images (not shown; see below for a quantitative determination). However, elimination of only these two NH_2-terminal lysines did not impair endocytosis in response to monensin (Fig. 6*D*). With regard to the individual contribution of the COOH-terminal lysines to the monensin effect, endocytosis of the lysine 577 (Fig. 6*E*, K577R) and 581 (Fig. 6*F*, K581R) mutants could not be distinguished clearly from that of the wild type construct in immunofluorescence assays. However, the lysine 619 mutant behaved like the 3KR mutant (Fig. 6*G*), indicating that this was the most important lysine involved in the constitutive endocytosis of the transporter. Indeed, reintroducing this lysine in the 3KR mutant restored transporter internaliza-

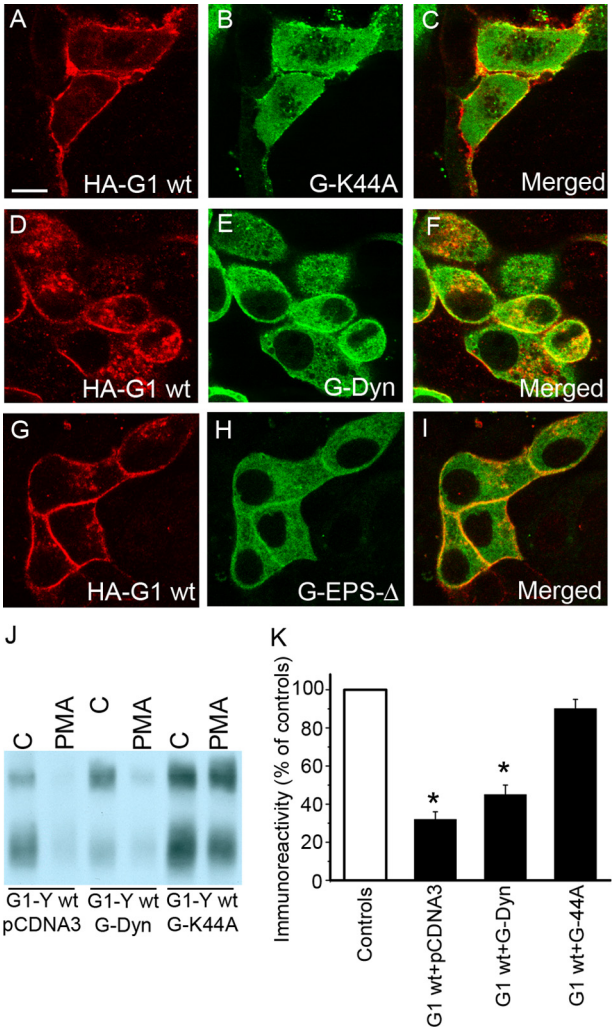

FIGURE 4. **PMA and monensin promote the internalization of GLYT1 through the dynamin 2-clathrin pathway.** MDCK cells were transfected with HA-GLYT1b (*HA-G1 wt*) plus GFP-dynamin 2 mutant K44A (*G-K44A*) (*A–C*), HA-GLYT1b plus GFP-dynamin 2 (*G-Dyn*) (*D–F*), or HA-GLYT1b plus GFP-EPS15Δ (*G-EPS-Δ*) (*G–I*). Two days after transfection, they were exposed to PMA and monensin, as indicated in the legend to Fig. 1. After treatment, the cells were fixed with 4% paraformaldehyde, immunostained, and analyzed by confocal microscopy. Note the blockade of endocytosis of the transporter in *A* and *G* but not in *D*. *Scale bar*, 15 μm. *J*, MDCK cells were transfected with the wild type GLYT1b-YFP (*G1-Y wt*), pCDNA3, GFP-Dyn2, and GFP-Dyn2 K44A in the combinations indicated in the figure. After 2 days, the cells were treated with vehicle alone (*C*) or with 1 μM PMA. The cell surface proteins were labeled with sulfo-NHS-biotin, and the biotinylated proteins were isolated with streptavidin-agarose beads and analyzed by immunoblotting with anti-GLYT1 antibodies. *K*, densitometry of immunoreactive bands, performed as in Fig. 2*C*. The results represent the means ± S.E. of three experiments, and they are presented as the percentage of the controls. Values were compared with controls by using Student's *t* test. *, $p < 0.001$.

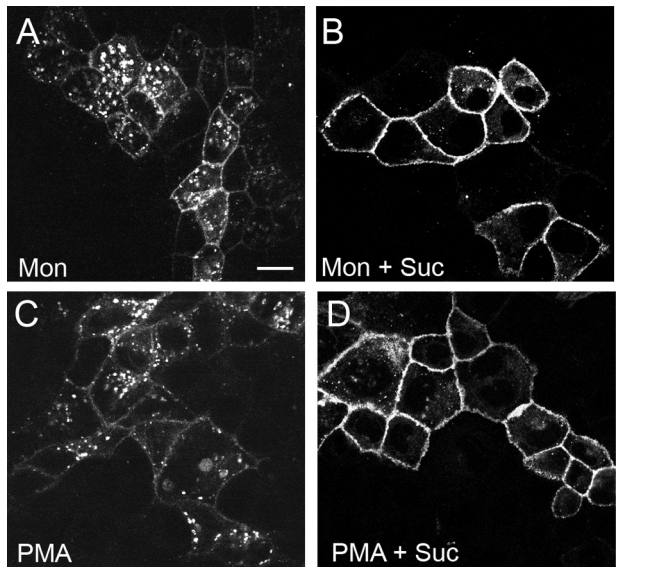

FIGURE 5. **Endocytosis of GLYT1b-YFP is impaired by hypertonic sucrose.** MDCK cells transfected with GLYT1b-YFP were incubated with monensin 10 μM (*A* and *B*) or with PMA 1 μM (*C* and *D*) to promote its internalization (compare with untreated control in Fig. 1). Where indicated, the cells were preincubated with sucrose (0.4 M, 30 min) (*Suc* in *B* and *D*) prior to the addition of monensin or PMA. The cells were then fixed and analyzed by confocal microscopy (*scale bar*, 15 μm).

tion to levels comparable with that of the wild type (Fig. 6*H*). A quantitative estimate of the effect of these mutations on the constitutive endocytosis of GLYT1b was obtained by measuring [^{3}H]glycine uptake after the addition of monensin (Fig. 6*I*). In comparison with the respective untreated controls, only mutation of Lys^{619} significantly reduced the effect of monensin, and in accordance with the fluorescence assays, reintroduction of this lysine into a 3KR mutant background restored the effect of monensin on glycine uptake. Similar quantitative results were obtained by measuring the amount of GLYT1b at the cell surface, as evaluated in a biotinylation assay quantified by densitometry (Fig. 6*J*).

The 3KR mutant of GLYT1b-YFP was also resistant to endocytosis in response to PMA (Fig. 7*C*; compare with controls in Fig. 8, *A* and *B*), although some vesicles were again evident in confocal planes close to the apical surface of MDCK cells, as in constitutive internalization (data not shown). Indeed, endocytosis of the 5KR mutant in response to PMA was weaker than that of the 3KR mutant (Fig. 7*D*; see Fig. 8 for a quantitative estimate). Similarly, elimination of the two NH_2-terminal lysines alone was insufficient to impair the endocytosis in response to PMA (Fig. 7*E*). With regard to the individual mutations in the COOH terminus, although the Lys^{577} and Lys^{581} mutations had an undetectable effect in immunofluorescence assays (Fig. 7, *F* and *G*, respectively), elimination of lysine 619 reduced endocytosis to a level similar to that of the 3KR mutant (Fig. 7*H*). Hence, this lysine appears to be the most important of the three for PMA-regulated internalization, as for constitutive endocytosis. Indeed, reintroduction of this lysine in the context of the 3KR construct again restored the PMA-dependent endocytosis (Fig. 7*I*).

A quantification of the contribution of these lysines to transporter endocytosis was obtained by measuring [^{3}H]glycine uptake after transfection of the diverse mutants and treatment with PMA. Although this treatment reduced the activity of WT GLYT1b by 55 ± 4%, it only reduced the activity of the 5KR and 3KR mutant by 16 ± 2 and 30 ± 5%, respectively (Fig. 8*A*). In accordance with the immunofluorescence assays, mutation of lysine 619 was as effective as the elimination of all three COOH-terminal lysines in abrogating the effects of PMA, whereas the effect of eliminating lysines 577, 581, and 25/26 was smaller, although not negligible (Fig. 8*A*). The decrease in transporter activity produced by PMA was mirrored by a decrease in the

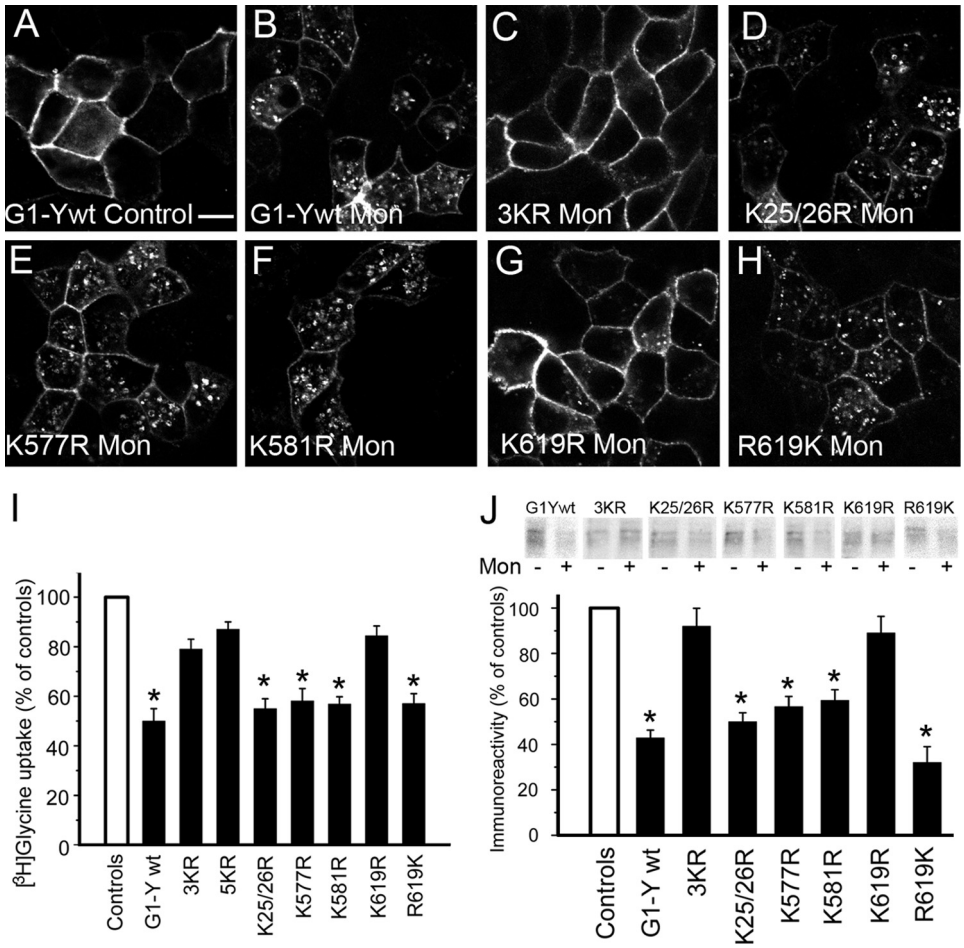

FIGURE 6. **The role of lysines in constitutive endocytosis of GLYT1b-YFP.** MDCK cells were transfected with the wild-type GLYT1b-YFP (*G1-Y wt* in *A* and *B*), with GLYT1b-YFP in which the three COOH-terminal lysines were mutated to arginine (*3KR* in *C*), with GLYT1b-YFP mutated at the two NH_2-terminal lysines (*K25/26R* in *D*), with the construct in which lysine 577 (*K577R* in *E*), lysine 581 (*K581R* in *F*), or lysine 619 (*K619R* in *G*) had been mutated, or with a construct where lysine 619 had been reintroduced into the 3KR mutant (*R619K* in *H*). Two days later, the cells were treated with vehicle alone (*Control* in *A*) or with 10 μM monensin (*Mon* in *B–H*), and they were then fixed and visualized by confocal microscopy. To simplify the figure, only the wild-type control is displayed. The rest of controls were similar to that one. *Scale bar*, 15 μm. *I*, [^{3}H]glycine uptake was measured for 10 min in MDCK cells that had been transfected with GLYT1-YFP or with the mutants indicated. The cells were pretreated with the vehicle alone (*Controls*, *open bar*) or with monensin (10 μM) for 30 min before performing the uptake assay (*closed bars*). The results represent the means ± S.E. of three triplicate experiments, and they are presented as the percentage of the untreated controls. *J*, MDCK cells were transfected with the constructs indicated, and after 2 days, the cells were treated with the vehicle alone (−) or monensin 10 μM (+) before the cell surface proteins were labeled with sulfo-NHS-biotin. The biotinylated proteins were isolated with streptavidin-agarose beads, and they were analyzed by immunoblotting with anti-YFP antibodies. For simplicity, only the monomer bands are presented. Immunoreactivity was quantified by densitometry, and the values are represented as the percentage of the respective control. Values are means ± S.E. of three experiments and were compared with control values by using Student's *t* test. *, $p < 0.001$.

amount of protein at the cell surface, as evaluated in biotinylation assays quantified by densitometry (Fig. 8*B*). Thus, although PMA treatment diminished the wild type biotinylated transporter by about 60%, the reduction was less than 12% for the 3KR, 5KR, and K619R constructs. Smaller contribution of Lys^{577} and Lys^{581} was also detected. Consistently with uptake and immunofluorescence experiments, reintroduction of Lys^{619} restored completely the endocytosis of the biotinylated transporter (Fig. 8*B*). In view of the central role played by lysine 619 in mediating both monensin and PMA effects, we performed a deeper study of the kinetic parameters of glycine uptake of mutants in this residue. Results presented in Table 1 reveal that its mutation to arginine reduced the V_{max} in response to either monensin or PMA, whereas its reintroduction in the context of the 3KR mutant largely restored that parameter. However, K_m was not significantly affected by these manipulations.

Ubiquitination Is Required for PMA-dependent Endocytosis of GLYTb—Since lysines are known to be the target of ubiquitin ligases, we studied the possible involvement of ubiquitination in the endocytosis of GLYT1b in response to both monensin and PMA. Accordingly, we took advantage of a ubiquitin-defective cell line, ts20, which carries a temperature-sensitive mutation in the E1 ubiquitin-activating enzyme. Monensin decreased the activity of the transfected GLYT1b by 53% in uptake assays performed over 10 min at 37 °C in cells that had grown at the permissive temperature (30 °C), whereas PMA decreased GLYT1b activity by 47% (Fig. 8*C*). These effects were diminished to 22 and 18%, respectively, in cells that had been preincubated at the restrictive temperature (40 °C, 6 h) prior to carrying out the transport assay, suggesting that the effects of both monensin and PMA were dependent on ubiquitination (Fig. 8*C*). Moreover, we found evidence of GLYT1b ubiquitination in Western blots of GLYT1b-YFP immunoprecipitated from transfected cells and probed with anti-ubiquitin antibodies (Fig. 9*A*). When compared with mock-transfected cells, proteins immunoprecipitated by the anti-GFP antibody displayed a smeared pattern of ubiquitinated protein. Notably, the amount of ubiquitin increased following pretreatment of the transfected cells with PMA, and the ubiquitinated protein was more prominent in the part of the blots that might correspond to GLYT1b oligomers (region around 200 kDa in Fig. 9*A*, *lane 6*). Treatment with PMA also decreased [^{3}H]glycine transport by endogenous GLYT1b by 45 ± 3% in the glioblastoma cell line C6. A correlation between the decrease in transport promoted for by PMA and an increase in ubiquitination was also observed in this cell line (Fig. 9*B*, *lane 4*).

We could not rule out the possibility that the ubiquitin detected in these experiments was incorporated into a protein that was associated with GLYT1b and that co-precipitated with the transporter. To address this issue, cells were co-transfected

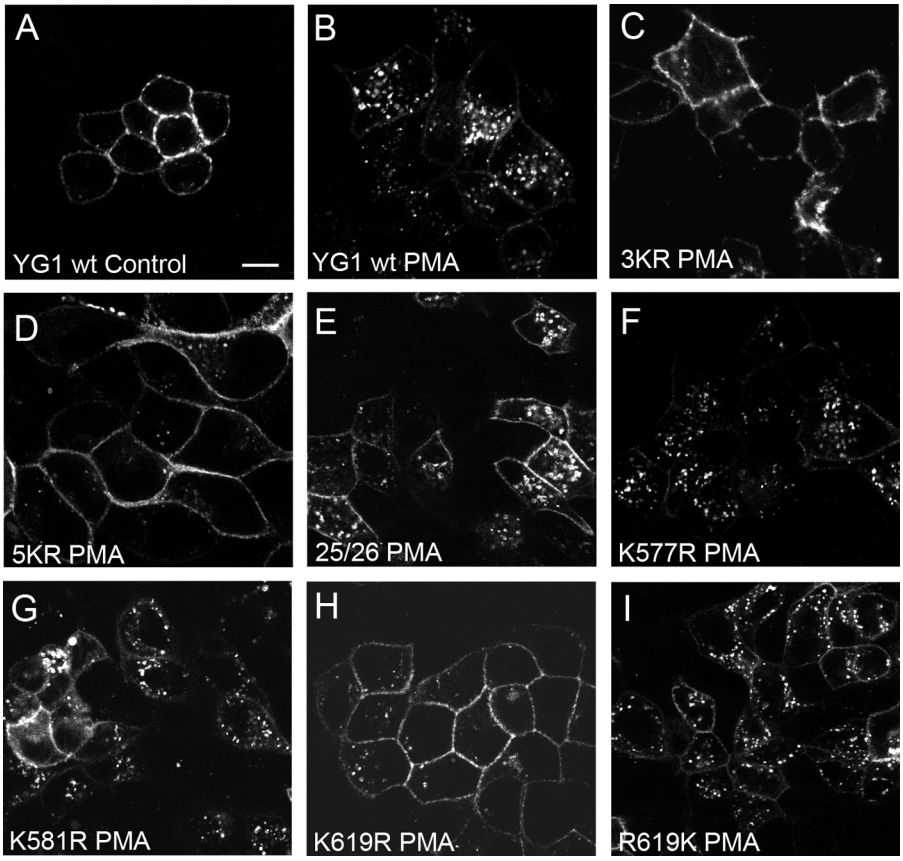

FIGURE 7. **The role of lysines on the intracellular distribution of GLYT1-YFP in response to PMA.** MDCK cells were transfected with the constructs indicated (see Fig. 7), and 2 days later, the cells were exposed to the vehicle alone (*Control* in *A*) or PMA (1 μM) for 30 min (*B–I*). The cells were then fixed and analyzed by confocal microscopy. To simplify the figure, only the wild-type control is displayed. The rest of controls were similar to that one. *Scale bar*, 15 μm.

with His_6-tagged ubiquitin and GLYT1b-YFP, and the transfected cells were solubilized under strong denaturing conditions (6 M guanidinium HCl) to ensure that associated proteins were removed. The putative GLYT1b-YFP-His-Ub conjugates were isolated by nickel chromatography (Ni^{2+}-nitrilotriacetic acid-agarose columns) and analyzed by immunoblotting after elution with imidazole (Fig. 9*C*). Although the signals in the immunoblots were quite faint, a GLYT1b-YFP-immunoreactive band of the expected size for the GLYT1b-YFP monomer was consistently detected (any oligomers pulled down would have been dissociated by guanidinium HCl). In addition, the amount of ubiquitinated transporter isolated increased after PMA treatment, producing a smeared band indicative of a heterogeneous mixture of ubiquitinated forms of GLYT1b (Fig. 9*C*, *lanes 5* and *6*). However, this was not the case for the 5KR mutant (Fig. 9*C*, *lanes 7* and *8*). Together, these data suggest a relationship between ubiquitination of GLYT1b and its endocytosis, either by the constitutive or regulated clathrin-dependent pathways, revealing the importance of lysine 619 in this process.

DISCUSSION

Several studies have shown that the glycine transporter GLYT1b is down-regulated by activation of protein kinase C in different cell systems (16–18). These experiments suggested that this down-regulation might be associated with the trafficking of the transporter, although the molecular mechanisms behind this process remained unexplored. Because GLYT1 is a major regulator of the concentration of glycine both at inhibitory and excitatory synapses, it represents a target for potentially important drugs with antipsychotic and analgesic properties (6). Thus, we have further investigated the mechanisms involved in the endocytic trafficking of this transporter. First, we have shown that the protein is subjected to both constitutive and PMA-regulated trafficking from the plasma membrane to the early/recycling endosomes. Constitutive endocytosis was revealed in the presence of monensin, a carboxylic ionophore previously used by other authors to that end (20, 30–33). Because this ionophore might have additional effects on other aspects of the intracellular traffic, we confirmed the existence of a constitutive endocytosis pathway by using a chimeric protein formed by the extracellular and transmembrane domains of the p75 NGFR fused to the full-length GLYT1b. Both constitutive and regulated endocytosis depend on the dynamin 2-clathrin pathway and could be blocked by a dominant negative mutant of dynamin 2 (K44A), by treatment with hypertonic sucrose or by co-transfection with Eps15Δ (that produces a dominant negative effect on the clathrin pathway) (34). This transporter contains two dileucine motifs in the COOH terminus of the protein that were previously implicated in basolateral sorting of the protein in polarized cells (14). Since this structural motif is thought to be a platform for the recruitment of clathrin during the endocytosis of several proteins (35), we first investigated the capacity of the dileucine motifs of GLYT1b to mediate the endocytosis. However, we did not find a major effect of these motifs in the endocytosis of the full-length protein. Thus, since ubiquitination has been implicated in the regulated endocytosis of various membrane proteins, including the neurotransmitter transporters for dopamine and glutamate (20–24, 26), we studied whether the constitutive and the regulated internalization of GLYT1b might depend on its ubiquitination. Site-directed mutagenesis revealed that both endocytic pathways rely on intracellular lysines, lysine 619 being the most relevant residue in this process, although mutation of the other COOH- and NH_2-terminal lysines also exerts a smaller effect on the endocytosis of GLYT1b. Indeed, lysine residues located in the intracellular tail of membrane proteins are common targets for ubiquitin recruitment, and these sites

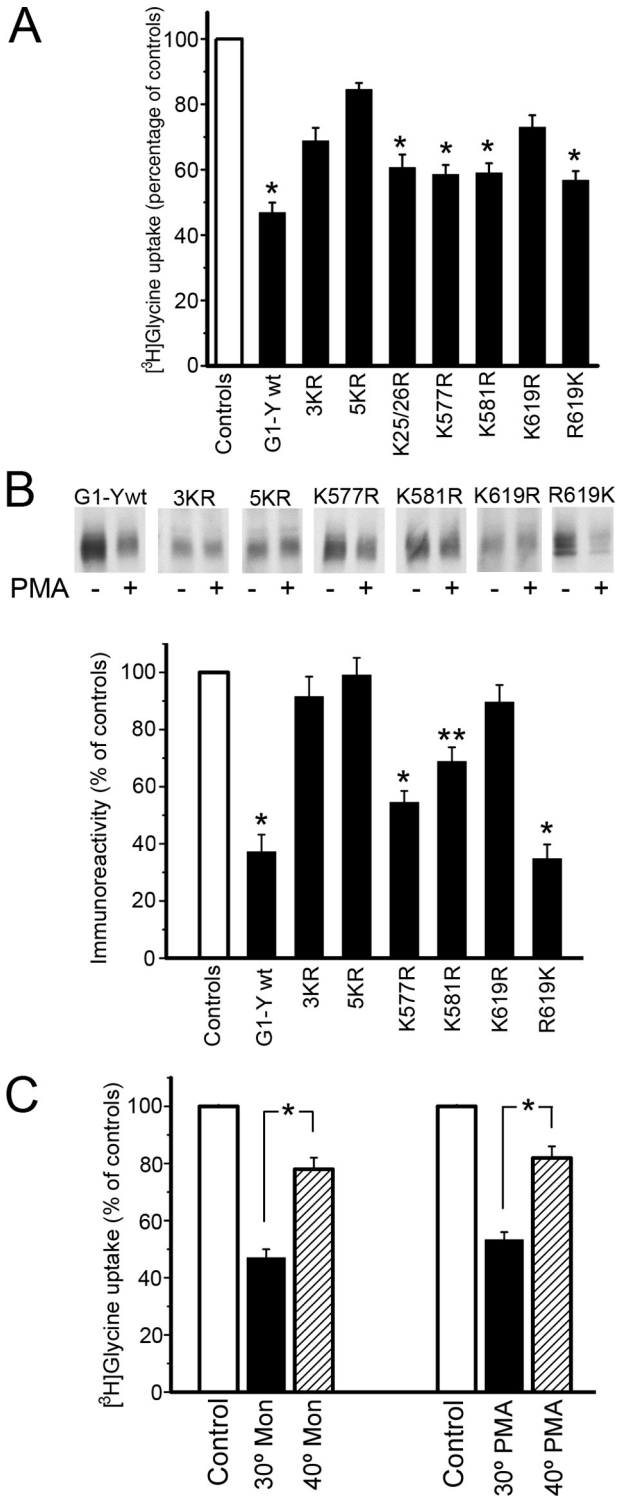

FIGURE 8. **Quantitative analysis of the effect of PMA and the influence of ubiquitination on GLYT1b endocytosis.** *A*, [^{3}H]glycine uptake was measured for 10 min in MDCK cells that had been transfected with GLYT1b-YFP (*G1-Y wt*) or with the mutants indicated. The cells were pretreated with the vehicle alone (*Controls*, *open bar*) or PMA (1 μM) for 30 min (*closed bars*) before the uptake assay was carried out. The results represent the means ± S.E. of three triplicate experiments, and they are presented as the percentage of the controls. *B*, MDCK cells were transfected with the constructs indicated, and after 2 days, the cells were treated with the vehicle alone (−) or PMA 1 μM (+) before the cell surface proteins were labeled with sulfo-NHS-biotin. The biotinylated proteins were isolated with streptavidin-agarose beads, and they were analyzed by immunoblotting with anti-YFP antibodies. For simplicity, only the monomer band is presented. Immunoreactivity was quantified by densitometry, and the values are represented as a percentage of the respective control. Values are means ± S.E. of three experiments. *C*, Ts20 cells were transfected with GLYT1b-YFP and maintained for 2 days at 30 °C. Half of the cells were maintained at 30 °C for 6 h before the uptake assay was performed, whereas the other half were kept at 40 °C. Cells were transferred to 37 °C and treated with monensin or PMA for 30 min. [^{3}H]glycine uptake was measured in controls and in heat-shocked cells for 10 min as indicated in *A*. The results represent the means ± S.E. of three triplicate experiments (*, $p < 0.001$; **, $p < 0.005$).

TABLE 1

K_m and V_{max} values for [^{3}H]glycine uptake in various GLYT1b constructs in response to monensin and PMA

[^{3}H]Glycine uptake was measured for 6 min in MDCK cells that had been transfected with the indicated GLYT1b constructs. The cells were pretreated with the vehicle alone (controls), with monensin (10 μM), or with PMA (1 μM) for 30 min before performing the uptake assay. The results represent the means ± S.E. of three triplicate experiments and represent the means ± S.E. of two triplicate experiments. Values were compared with control values by using Student's *t* test.

Construct/Treatment	K_m	V_{max} (percentage of control values)
	μM	*nmol/6 min/mg protein*
GLYT1b wild type		
Control	278 ± 20	5.53 ± 0.24 (100%)
Monensin	285 ± 48	3.15 ± 0.40 (57%)[a]
PMA	249 ± 41	3.03 ± 0.28 (54%)[a]
K619R		
Control	229 ± 25	4.64 ± 0.17 (100%)
Monensin	293 ± 69	3.89 ± 0.24 (85%)
PMA	197 ± 44	4.13 ± 0.26 (89%)
R619K		
Control	238 ± 47	4.87 ± 0.19 (100%)
Monensin	244 ± 38	2.53 ± 0.26 (52%)[a]
PMA	185 ± 35	2.39 ± 0.22 (49%)[a]

[a] $p < 0.001$.

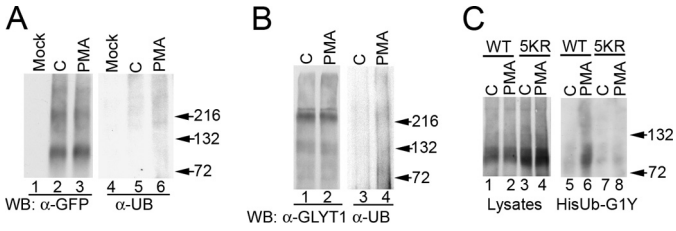

FIGURE 9. **Ubiquitination of GLYT1b.** *A*, MDCK cells were transfected with GLYT1b-YFP, or they were mock-transfected, and then the cells were treated with the vehicle alone (*C*) or with PMA (1 μM; *PMA*) for 30 min. The cell extracts were immunoprecipitated with anti-YFP antibodies, and the material recovered was resolved by SDS-PAGE and immunoblotted. The immunoblots were probed with anti-ubiquitin antibodies (*WB*: α*UB*; *lanes 4–6*) that were visualized by the ECL method before the blots were reprobed with anti-GFP (*WB*: α*GFP*; *lanes 1–3*). *B*, C6 cells were treated with the vehicle alone (*C*) or with PMA (1 μM) for 30 min, and the cell extracts were then immunoprecipitated with anti-GLYT1 antibodies, resolved by SDS-PAGE, and immunoblotted. The immunoblots were probed with anti-ubiquitin antibodies (*WB*: α*UB*; *lanes 3* and *4*) and visualized by the ECL method. The blots were reprobed with anti-GLYT1 (*WB*: α*GLYT1*, *lanes 1* and *2*). *C*, cells were transfected with His-ubiquitin plus GLYT1b-YFP (*WT*) or plus the 5KR mutant and treated with vehicle alone (*C*) or with PMA. After solubilization, His-Ub conjugates were isolated with nickel-agarose beads, eluted from the beads, resolved by SDS-PAGE, and immunoblotted with anti-GFP antibodies (*lanes 5–8*). To control the efficiency of transfection, a sample of the lysates (*lanes 1–4*) was also analyzed with anti-GFP antibodies.

are normally redundant (19). However, because the 5KR mutant still undergoes residual endocytosis in response to PMA and to monensin, it is possible that additional lysines in the intracellular loops might also participate in these events, although alternative endocytosis pathways (*e.g.* raft-dependent) might account for this phenomenon.

GLYT1b immunoprecipitated from both transfected MDCK cells and the C6 glial cell line that expresses native GLYT1b

incorporated ubiquitin, and the amount of ubiquitin incorporated increased in response to PMA. Although this ubiquitin might be incorporated to an associated protein that co-immunoprecipitates with GLYT1b, this seems unlikely due to the strongly denaturating protocol used to recover the GLYT1b-YFP-His-Ub, which should dissociate GLYT1b from any interacting protein. Moreover, the site-directed mutagenesis data represent further evidence of the direct ubiquitination of intracellular lysines.

Although various studies have addressed the role of ubiquitination in PMA-regulated endocytosis of membrane transporters, less is known about the importance of ubiquitination for their constitutive endocytosis. Because under basal conditions or in the presence of monensin there is only a faint ubiquitination signal in Western blots, we could not measure the differences in ubiquitination of the various GLYT1b mutants. However, the common dependence on Lys^{619} of both regulated and constitutive internalization is consistent with constitutive endocytosis, being also dependent on ubiquitination. Moreover, the endocytic process was largely inactivated in the ts20 cell line at restrictive temperatures. Analysis of the stability of the protein in the presence of cycloheximide indicates that GLYT1b is stable for several h, whereas in the presence of monensin, the transporter appears to be removed from the cell surface. Hence, it would appear that the constitutively endocytosed transporter must be recycled back to the cell surface, a possibility that is reinforced by the co-localization of the internalized protein with transferrin, a marker of the recycling endosomes. This situation is reminiscent of the behavior of the epidermal growth factor receptor, a fraction of which was recently shown to be endocytosed through the clathrin pathway and then recycled to the cell surface, whereas another fraction was endocytosed through a clathrin-independent pathway and degraded in lysosomes (36). Since the steady state amount of ubiquitinated protein seems to be rather small, there must be also an efficient system to remove ubiquitin, permitting the return of the protein to the plasma membrane rather than its targeting to lysosomes. A similar turnover mechanism is known to occur for the epithelial sodium channel, which is recycled after ubiquitin removal by UCH-L3 (37).

Our data suggest that activation of the PKC pathway increases the rate of ubiquitin incorporation to the target lysine(s), although differences must exist with the constitutive endocytosis mechanism, since a fraction of the protein is destined for degradation after the PMA treatment rather than being recycled. It is possible that under basal conditions, these lysines are partially occluded and that they only become fully exposed after activation of PKC, which might induce a conformational change in the transporter. The very fast constitutive endocytosis of the short NG1ct-wt chimera is consistent with this interpretation. Indeed, since endocytosis of this chimera was not accelerated by PMA (data not shown), the lysines in NG1ct-wt might already be fully exposed to the ubiquitination machinery. The ubiquitin ligases that modify GLYT1b remain to be identified, and although a single ligase might be responsible for both constitutive and regulated ubiquitination, each process might alternatively be driven by a specific ubiquitin ligase. It is also unclear if direct phosphorylation of the transporter is required for PMA-mediated endocytosis, since mutation of all of the consensus PKC phosphorylation sites does not impair the down-regulation of transporter activity (18). Thus, phosphorylation might occur at a non-consensus site, or phosphorylation of either the ubiquitin ligase or other associated proteins may be required rather than that of the transporter itself. The relationship between ubiquitination and PKC-dependent phosphorylation also remains unclear for DAT, since elimination of the potential PKC targets in this transporter does not prevent its internalization (38). Hence, again there does not appear to be a cause-effect relationship between phosphorylation and ubiquitination for this transporter. Likewise, the role of phosphorylation in ubiquitin-dependent endocytosis of the glutamate transporter GLT1 remains unclear (24, 26).

In summary, these results indicate that GLYT1b undergoes active turnover from the plasma membrane to the recycling endosome, a process that is accelerated by activation of the protein kinase C. The data support a major contribution of the clathrin-dependent pathway to both the constitutive and the regulated endocytosis of this transporter. In addition, we present evidence that ubiquitin is incorporated into GLYT1b both under basal conditions and after PKC activation. We also show that the lysine 619 in the carboxyl terminus of GLYT1b is essential for constitutive and regulated endocytosis of the protein. It remains to be determined whether the normal recycling of GLYT1b may be altered in pathologies in which the ubiquitination system is affected, thereby interfering with its function in inhibitory and excitatory neurotransmission.

Acknowledgments—We thank E. Núñez for expert technical help and Carlos Sánchez in the confocal microscopy department of the Centro de Biología Molecular "Severo Ochoa." We also thank Dr. G. Dechant for the NGFR plasmid, Dr. M. A. Alonso for dynamin 2 and Eps15 plasmids, and Dr. H. Cabedo for ts20 cells.

REFERENCES

1. Betz, H., Gomeza, J., Armsen, W., Scholze, P., and Eulenburg, V. (2006) *Biochem. Soc. Trans.* **34,** 55–58
2. Kemp, J. A., and Leeson, P. D. (1993) *Trends Pharmacol. Sci.* **14,** 20–25
3. Zafra, F., and Giménez, C. (2008) *IUBMB Life* **60,** 810–817
4. Gomeza, J., Hülsmann, S., Ohno, K., Eulenburg, V., Szöke, K., Richter, D., and Betz, H. (2003) *Neuron* **40,** 785–796
5. Cubelos, B., Giménez, C., and Zafra, F. (2005) *Cereb. Cortex* **15,** 448–459
6. Sur, C., and Kinney, G. G. (2007) *Curr. Drug Targets* **8,** 643–649
7. Cubelos, B., González-González, I. M., Giménez, C., and Zafra, F. (2005) *J. Neurochem.* **95,** 1047–1058
8. Bergeron, R., Meyer, T. M., Coyle, J. T., and Greene, R. W. (1998) *Proc. Natl. Acad. Sci. U.S.A.* **95,** 15730–15734
9. Chen, L., Muhlhauser, M., and Yang, C. R. (2003) *J. Neurophysiol.* **89,** 691–703
10. Kinney, G. G., Sur, C., Burno, M., Mallorga, P. J., Williams, J. B., Figueroa, D. J., Wittmann, M., Lemaire, W., and Conn, P. J. (2003) *J. Neurosci.* **23,** 7586–7591
11. Yee, B. K., Balic, E., Singer, P., Schwerdel, C., Grampp, T., Gabernet, L., Knuesel, I., Benke, D., Feldon, J., Mohler, H., and Boison, D. (2006) *J. Neurosci.* **26,** 3169–3181
12. Gabernet, L., Pauly-Evers, M., Schwerdel, C., Lentz, M., Bluethmann, H., Vogt, K., Alberati, D., Mohler, H., and Boison, D. (2005) *Neurosci Lett.* **373,** 79–84
13. Tsai, G., Ralph-Williams, R. J., Martina, M., Bergeron, R., Berger-Sweeney, J., Dunham, K. S., Jiang, Z., Caine, S. B., and Coyle, J. T. (2004) *Proc. Natl.*

Acad. Sci. U.S.A. **101,** 8485–8490
14. Poyatos, I., Ruberti, F., Martínez-Maza, R., Giménez, C., Dotti, C. G., and Zafra, F. (2000) *Mol. Cell Neurosci.* **15,** 99–111
15. Melikian, H. E., and Buckley, K. M. (1999) *J. Neurosci.* **19,** 7699–7710
16. Gomeza, J., Zafra, F., Olivares, L., Giménez, C., and Aragón, C. (1995) *Biochim. Biophys. Acta* **1233,** 41–46
17. Morioka, N., Abdin, J. M., Morita, K., Kitayama, T., Nakata, Y., and Dohi, T. (2008) *Neurochem. Int.* **53,** 248–254
18. Sato, K., Adams, R., Betz, H., and Schloss, P. (1995) *J. Neurochem.* **65,** 1967–1973
19. Miranda, M., and Sorkin, A. (2007) *Mol. Interv.* **7,** 157–167
20. Sorkina, T., Hoover, B. R., Zahniser, N. R., and Sorkin, A. (2005) *Traffic* **6,** 157–170
21. Sorkina, T., Miranda, M., Dionne, K. R., Hoover, B. R., Zahniser, N. R., and Sorkin, A. (2006) *J. Neurosci.* **26,** 8195–8205
22. Miranda, M., Dionne, K. R., Sorkina, T., and Sorkin, A. (2007) *Mol. Biol. Cell* **18,** 313–323
23. Miranda, M., Wu, C. C., Sorkina, T., Korstjens, D. R., and Sorkin, A. (2005) *J. Biol. Chem.* **280,** 35617–35624
24. Sheldon, A. L., González, M. I., Krizman-Genda, E. N., Susarla, B. T., and Robinson, M. B. (2008) *Neurochem. Int.* **53,** 296–308
25. Hatanaka, T., Hatanaka, Y., and Setou, M. (2006) *J. Biol. Chem.* **281,** 35922–35930
26. González-González, I. M., García-Tardón, N., Giménez, C., and Zafra, F. (2008) *Glia* **56,** 963–974
27. Hershko, A., and Ciechanover, A. (1998) *Annu. Rev. Biochem.* **67,** 425–479
28. Fernández-Sánchez, E., Díez-Guerra, F. J., Cubelos, B., Giménez, C., and Zafra, F. (2008) *Biochem. J.* **409,** 669–681
29. Olivares, L., Aragón, C., Giménez, C., and Zafra, F. (1995) *J. Biol. Chem.* **270,** 9437–9442
30. Potau, N., Bailey, A. C., Roach, E., Williams, J. A., and Goldfine, I. D. (1984) *Endocrinology* **115,** 205–213
31. Basu, S. K., Goldstein, J. L., Anderson, R. G., and Brown, M. S. (1981) *Cell* **24,** 493–502
32. Deken, S. L., Wang, D., and Quick, M. W. (2003) *J. Neurosci.* **23,** 1563–1568
33. Fournier, K. M., González, M. I., and Robinson, M. B. (2004) *J. Biol. Chem.* **279,** 34505–34513
34. Benmerah, A., Bayrou, M., Cerf-Bensussan, N., and Dautry-Varsat, A. (1999) *J. Cell Sci.* **112,** 1303–1311
35. Heilker, R., Spiess, M., and Crottet, P. (1999) *BioEssays* **21,** 558–567
36. Sigismund, S., Argenzio, E., Tosoni, D., Cavallaro, E., Polo, S., and Di Fiore, P. P. (2008) *Dev. Cell* **15,** 209–219
37. Butterworth, M. B., Edinger, R. S., Ovaa, H., Burg, D., Johnson, J. P., and Frizzell, R. A. (2007) *J. Biol. Chem.* **282,** 37885–37893
38. Granas, C., Ferrer, J., Loland, C. J., Javitch, J. A., and Gether, U. (2003) *J. Biol. Chem.* **278,** 4990–5000